Simulation of Combustion in SI-Engines under Unconventional Operating Conditions by Means of a Quasidimensional Model and Experimental Verification

M. Röder
FEV, Aachen

A. Brohmer
LAT Aachen Technical University

ABSTRACT:

A computer program simulating the SI-engine process including the prediction of the mass fraction burned by means of a quasidimensional model is described and validated by comparison of measured and calculated data. Investigations were carried out under varying, unconventional engine operating conditions. The range of reliability of this program with regard to exhaust gas recirculation, very lean mixture combustion and low engine speeds will be discussed.

INTRODUCTION:

As a consequence of the increasing demands on the internal combustion engine, numerical methods for the prediction and optimization of the combustion process are becoming more and more important. Apart from thermodynamic models which are commonly used with regard to the analysis of SI-engine processes, quasidimensional models have been developed for more detailed purposes. The parameters of these models are based on a few engine measurements only, but this method is a reasonable compromise requiring not too much computer capacity while being useful with regard to the prediction of the combustion rate under changing conditions. Multidimensional codes have been developed mainly for the analysis of air motion in the inlet manifolds and the combustion chamber as well as for studying the influence of swirl and squish on SI-combustion. However, these codes require a very large computation capacity. In addition, there is still a lack of proved capablity of completely predicting the process.

THE MODEL:

This paper presents the results obtained by a computer simulation model for SI-engines including a quasidimensional approach for the increase of the mass fraction burned . During combustion, the combustion chamber is divided into two zones separated from each other by the flame front which is assumed hemispherical. The rate of unburned gas entering the flame front area is calculated according to the entrainment model developed by Blizard and Keck /1/ as follows:

$$\frac{dm_E}{d\alpha} = \frac{1}{\omega} \rho_1 A_E u_E$$

with the density of unburned gas ρ_1 and the flame front area A_E. The entrainment velocity u_E is composed by the laminar flame speed and the turbulence velocity characterizing the eddy-motion state in the combustion chamber.

Assuming homogenous, isotropic turbulence in the combustion chambers investigated, the characteristic values describing the air motion in the flame front are calculated on the basis of the correlation between the turbulent kinetic energy k and the dissipation ε as shown in /1,2,3/ (k-ε-model). The mass fraction burned of the gas in the flame front is assumed to follow an exponential function with the characteristic time τ:

$$\frac{dm_2}{d\alpha} = \frac{1}{\omega} \frac{m_E - m_2}{\tau}$$

m_2: mass of the gas burned. The characteristic time τ is also used to calculate the combustion delay:

$$\alpha_{BV} = c_B \tau \omega$$

The model also covers the main chemical reaction processes as to the formation of nitric oxides and carbon monoxide in the burned gas. For the calculation of the heat losses, the Woschni heat transfer correlation is used. The computation of the combustion period is preceeded by the computation of the gas exchange period (constant pressure model) and the

compression period in order to determine the thermodynamic condition at ignition timing.
The correctness of the computer program has been checked by a large number of comparisons between measured and computed results, especially with regard to the validation of the approach for the laminar flame speed and the turbulence model. Investigations have been carried out using different fuels including ordinary gasoline. Starting with a disc-shaped combustion chamber, the program has been extended to more complicated geometries. The effects of squish on the turbulent air motion is taken into account as described by /3/.

After one single adaption of four parameters quantifying the turbulence level, the turbulence structure, the combustion delay and the squish flow, the model produces reliable results in the whole range of speed and load for the engine configuration considered. In general, this adaption can be done at any engine operating point. The parameters determined for the turbulence model are constant for all engine operating points; therefore only very few comparisons between measurement and prediction have to be carried out. The combustion delay parameter, however, shows a dependence on the load, thus this correlation has to be determined by help of several measurements. For this paper, the adaption was done for different loads at 1500 rpm and stoichiometric mixture with regard to best correspondence between measured and calculated mass fraction burned and cylinder pressure curve as well as to good correspondence between measured and calculated integral data such as efficiency, fuel consumption etc.

Some results obtained by the above described simulation model compared to measurements taken under various, unconventional conditions are discussed in the following. The measurements have been taken on a 1-cylinder test engine and a 4-cylinder production engine both equipped with a heron combustion chamber. Ignition timing is always chosen with regard to best fuel consumption.

SPEED REDUCTION:

Experimental investigations reveal that for part load the SI-engine efficiency at given engine power can be considerably improved by reducing the speed level. This is due to a better mechanical efficiency by lower friction of the engine and to a higher internal efficiency by reduction of the throttling losses.

The computation gives further information on the combustion process at low speeds; this will be discussed in the following by means of a comparison between the predicted combustion process and the analysis of pressure curves averaged over 200 consecutive cycles measured at constant load in the range of 600 rpm - 1500 rpm.

Fig. 1 shows a comparison between calculated and measured cylinder pressure and burned mass fraction for two speeds. In both cases, engine operation is at the same mean effective pressure. To gain

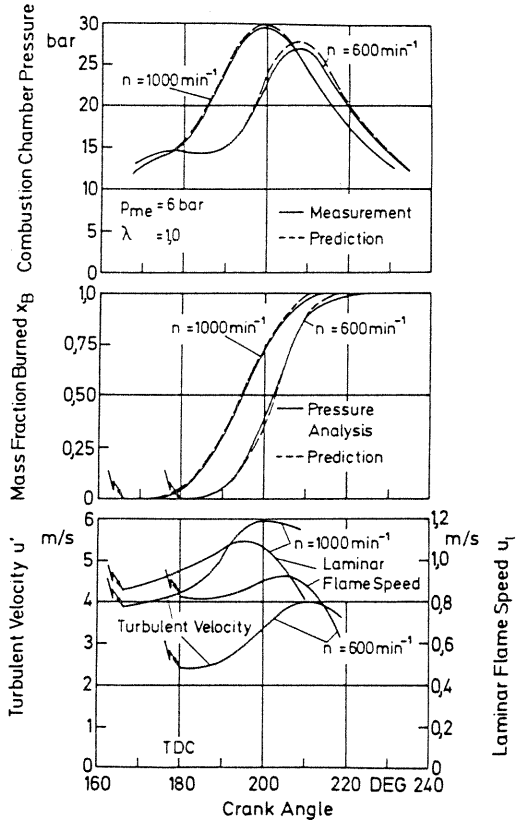

Fig. 1: Turbulent velocity, mass fraction burned and pressure curve at very low speed (comparison of measurment and prediction)

optimum fuel consumption, the spark timing has to be retarded considerably, thereby making use of the decreasing combustion duration in crank angle degrees (fig. 2). The heat losses to the combustion chamber walls can also be minimized by the retarded combustion period. Simulation calculations at normal speed in /1/ show that the heat losses to the walls are decreasing with a later ignition timing but at the expense of an increasing exhaust-gas enthalpy. When comparing the burned mass fraction curves for both speeds, it must be taken into account that the steeper curve at n=600 rpm does not correspond to a faster combustion since at low speeds the same intervals of crank angles correspond to longer time intervals.

The combustion delay parameter had to be adapted dependent on the engine load. The turbulence parameters could be kept constant over the entire speed range. The curves showing the turbulence velocity calculated for the combustion process at 600 and 1000 rpm with these constant parameters clearly indicate the decay of turbulence with lower speeds. At the same time, the laminar flame speed is also reduced by the slihtly lower pressure level and the higher residual gas fraction (see fig. 3) at 600 rpm. Both values correspond to the compression curve since they depend on pressure and temperature of the unburned mixture, which even leads to a slight reduction after the top dead center. As soon as the combustion starts, these velocities are distinctly increasing.

Fig. 2 shows the correlation between the maximum values of these velocities and the engine speed. As expected, the

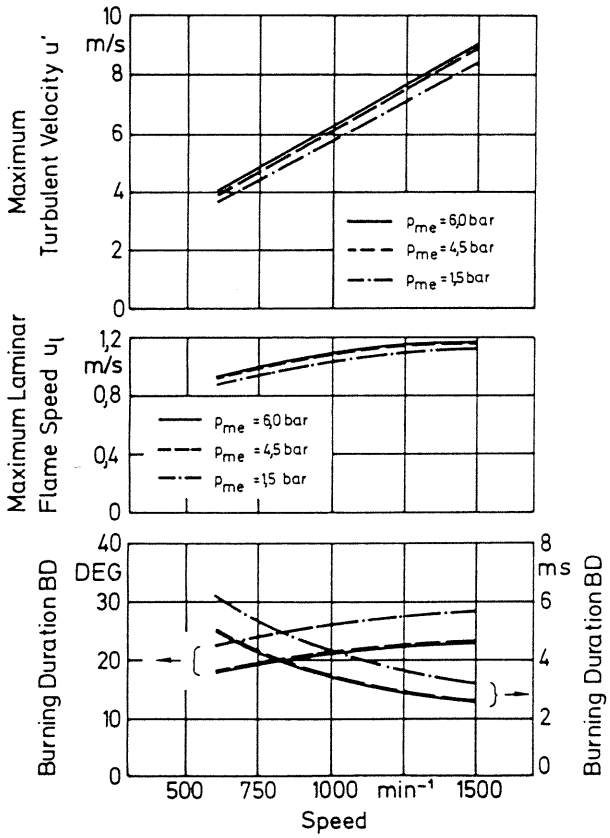

Fig. 2: Characteristic values of the combustion model at low speed and stoichiometric mixture

decreasing velocities correspond to longer combustion duration which is plotted both in angular intervals and in time intervals. Fig. 3 gives the residual gas fraction calculated and the maximum combustion pressures explaining the decrease in laminar flame speed. The

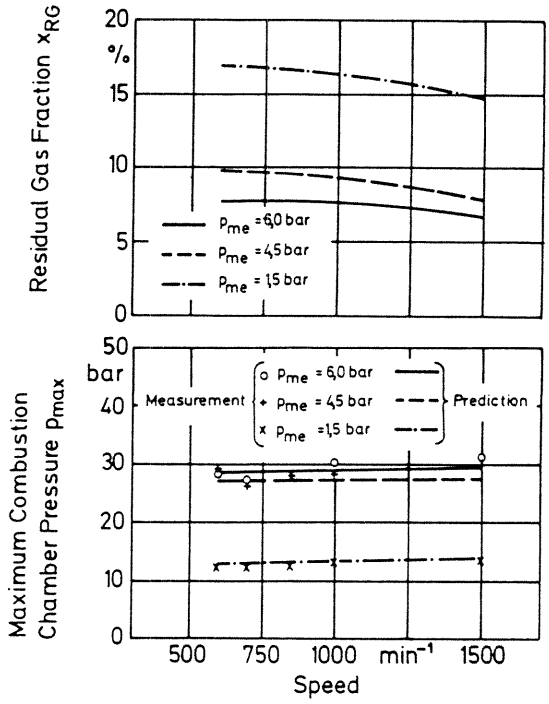

Fig. 3: Residual gas fraction and maximum pressure for constant loads at low speed and stoichiometric mixture

residual gas fraction is increasing when reducing the speed since there is more time for the exhaust-gas overflow during the valve overlap. The reduction of the pressure level at constant mean effective pressure is mainly induced by the lower mean indicated pressure due to less friction; the calculated tendency is compared to the values measured in the lower part of fig. 3.

Fig. 4 explains the decline in the internal efficiency at decreasing speed shown by means of the energy distribution in the range of 600 rpm to 1000 rpm. The energy fractions are related to the total fuel energy. The main reason of this decline is the increase of heat transfer through the cylinder walls at decreasing speed; the increasing blow-by quantity also affects the efficiency. As expected, the submodel for the heat transfer does yield an increase of heat losses at decreasing speed. The comparison between the curves of the two different loads reveals that the relative heat losses are strongly dependent on the engine load. Measured efficiencies are also shown in the same figure to give an additional verification of the simulation program.

LEAN MIXTURE COMBUSTION:

A possibility to reduce at the same time the fuel consumption and the nitric oxide emissions is given by operating the engine with very lean mixtures. By

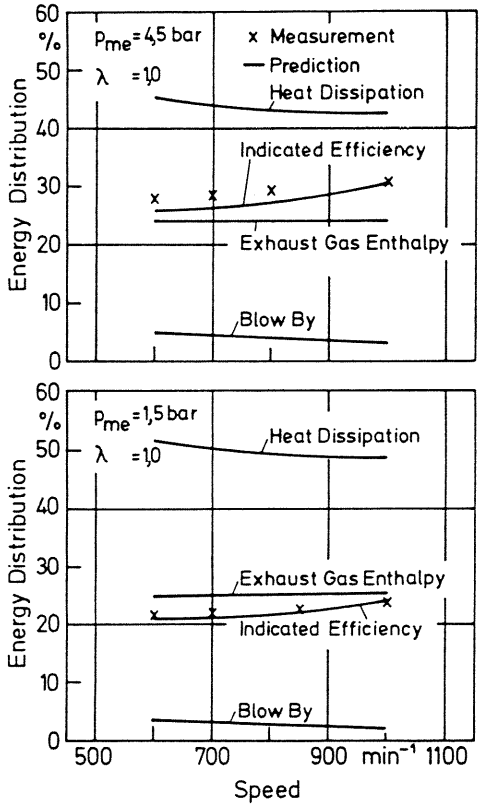

Fig. 4: Energy distribution at low engine speeds (related to total fuel energy)

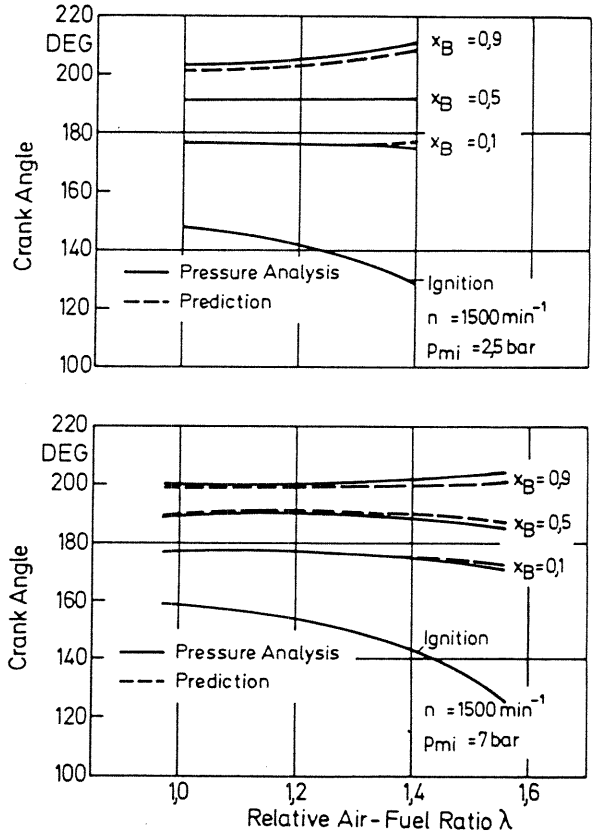

Fig. 5: Comparison between measured and predicted burned mass fraction x_B under very lean operation

optimization of the combustion chamber geometry and the charge motion, a relative A/F-ratio up to approximately λ=1.6 can be obtained /6/. Tests run on a 4-cylinder production engine with changing A/F-ratio at optimum spark timing have been carried out in order to prove the reliablity of the computation model under these operating conditions. The indicated pressure curve and the other values measured determine the mass fraction burned which will then be compared to the corresponding values predicted.

Fig. 5 gives the comparison between the calculated mass fraction burned and that one based on the indicated pressure for two different loads in the range of λ=1.0 almost until the misfire limit. The curves are corresponding to constant burned mass fraction values which describe characteristic sections of the combustion: x_B=10% is equivalent to the end of the combustion delay, x_B=50% is describing the center of the combustion period and the interval between x_B=10% and x_B=90% repesents the combustion duration. The model obviously simulates very well the combustion process even with extreme lean mixture. The longer combustion duration experimentally investigated is very well simulated. Discrepancies between the analysis of the pressure curve and the calculation are less than 5 degrees CA even towards the end of the combustion.

Fig. 6 shows the good correspondence of the values measured and calculated in the A/F-range considered. In the upper part, the pressure curves calculated and measured are given for 3 different A/F-ratios. The differences of maximum pressure are distinctly under 1 bar in the case of each operating point represented. In the middle, fig. 6 again gives a comparison of the mass fraction burned. There are slight differences of the combustion delay time between the curves calculated and measured but there is a very good correspondence in the range of 10% to 90% mass fraction burned which is decisive for the combustion; a discrepancy less than 1 degree CA is found at the combustion center (x_B=50%).

The reason for the obviously slower combustion in the case of very lean mixtures can easily be explained by the lower part of fig. 6. It shows the curves of the laminar flame speed obtained by using the approach according to /5/. In the case of lean mixtures, the laminar flame speed is clearly lower than in the case of stoichiometric mixtures. This requires an early ignition timing with lower pressure and

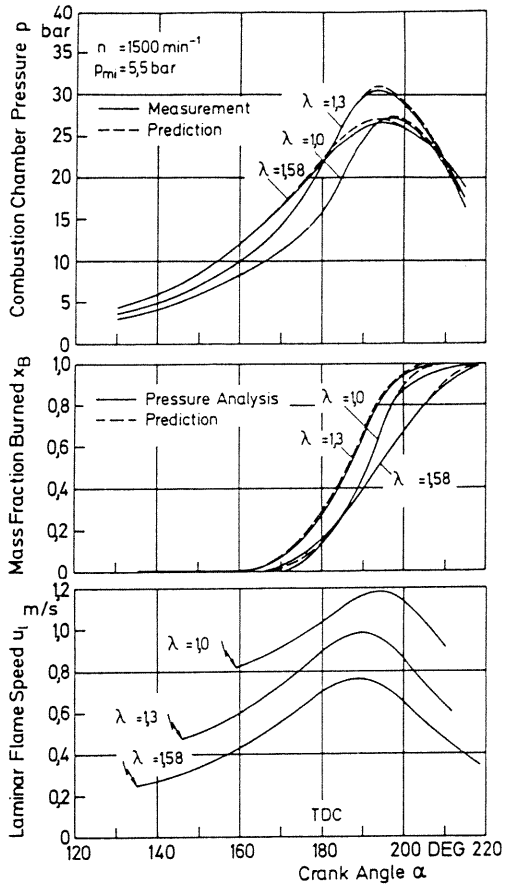

Fig. 6: Influence of lean mixture combustion on the SI-engine process

temperature, thus explaining the great decrease of laminar flame speed at the ignition timing towards the lean limit. Moreover, the slower combustion leads to a lower temperature level; consequently, with the leanest mixture, the laminar flame speed does not even exceed the lowest velocity computed for a relative A/F-ratio of $\lambda=1.0$. At the operating point represented (n=1500 rpm, pmi=5.5 bar), the maximum laminar flame speed decreases by appr. 35% and consequently causes a combustion duration longer by 33%.

Fig. 7 illustrates for three different loads the impact of the air-fuel ratio on the two velocities, laminar flame speed and turbulence velocity, which are essential for the entrainment velocity and thereby for the duration of the combustion. Towards leaner mixtures, both velocities are decreasing, the laminar flame speed considerably more than the turbulence velocity. The computation reveals that the curves of the turbulence velocity versus crank angle are nearly the same for all A/F-ratios until combustion starts. As shown in fig. 7, the differences of the maximum values result almost exclusively from a quicker combustion whereas the differences at ignition timing are due to

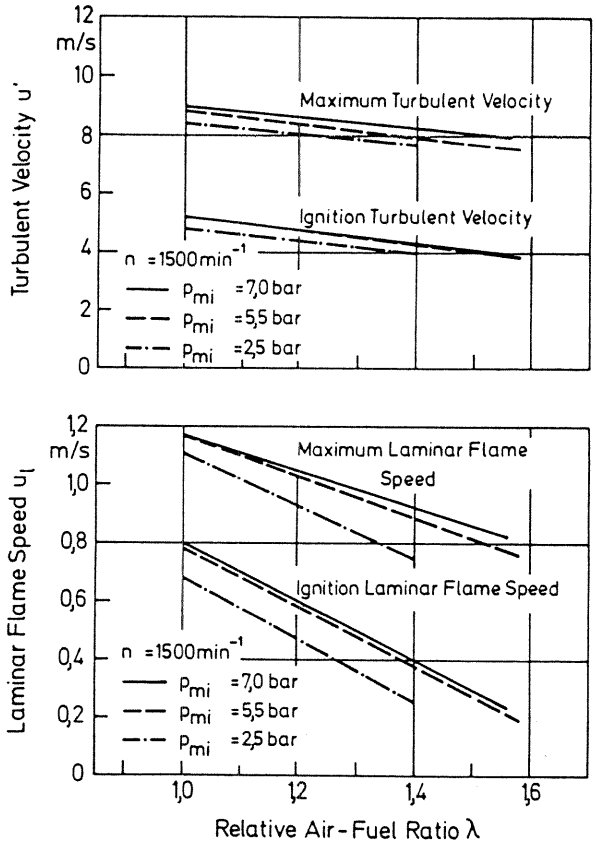

Fig. 7: Characteristic values of the combustion model versus air-fuel ratio

the different position of the ignition timing itself.

The nearly linear drop of maximum laminar flame speed and laminar flame speed at ignition timing with increasing A/F-ratios shows that the corresponding model describes very well a regular combustion. A misfire limit cannot be determined because only longer combustion durations are calculated for mixtures beyond the actual lean limit of the engine. This is also true for the

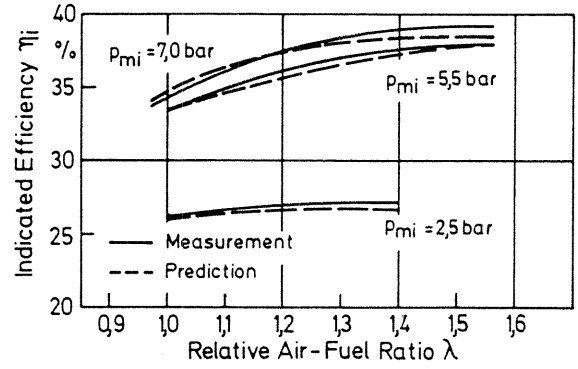

Fig. 8: Measured and calculated indicated efficiency under very lean operation

internal efficiency curve; a computational simulation of the abrupt drop beyond the lean operation limit is not possible by this model.
The efficiency gains at regular lean engine operation are clearly shown by the computation model. Fig. 8 represents the values measured and the efficiencies calculated. The small differences confirm that the model simulates quiet well the engine process.

EXHAUST GAS RECIRCULATION:

EGR is another possibility to reduce the nitric oxide emission of SI-engines. The portion of inertial gas to the cylinder charge is increased by adding exhaust gas to the fresh mixture. In the presented calculation model, this leads to a reduced laminar flame speed thus causing longer combustion durations.

The effect of EGR on pressure and temperature curve and the laminar flame speed is shown in fig. 9. In the upper part of fig. 9, the pressure curves are represented for three different operating points at recirculation rates of 0%, 10.4% and 20.8% related to total charge mass determined by means of the quasidimensional approach. Despite higher cylinder mass, the maximum pressure slightly falls with increasing recirculation rates because of the longer combustion durations. A comparison with the measured pressure curves shows a

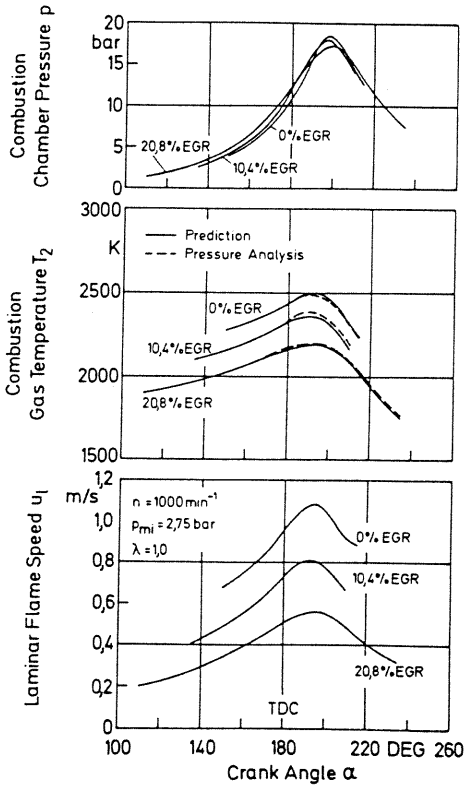

Fig. 9: Influence of EGR on the combustion process

maximum discrepancy of 1.5 bar for the peak pressure at the highest recirculation rate. In the middle of fig. 9, the good correspondence of the pressure analysis and the quasi-dimensional calculation is represented by the temperature curves of the combustion gas. In the lower part of fig. 9, the laminar flame speed is shown which is the main reason for the longer combustion durations. The maximum values are decreasing almost proportionally to the maximum temperature of the combustion gas. Moreover, the two lower figures clearly show the longer combustion durations (including the combustion delay) with the EGR.

Fig. 10 shows again a comparison between constant burned mass fraction values calculated on the basis of the pressure curve and by means of the quasidimensional model for the whole range of EGR. Up to a recirculation rate

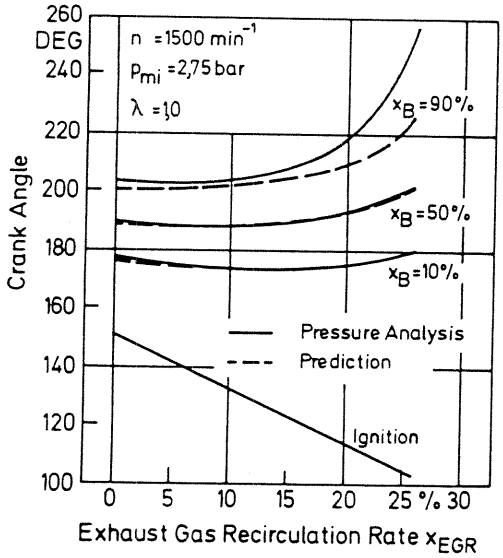

Fig. 10: Comparison between measured and predicted burned mass fractions x_B with EGR

of about 15% there are few discrepancies between analysis and prediction. Recirculation rates beyond 15% show an increase of discrepancies within the last combustion phase after about x_B=80%. Therefore, the 90%-curves are diverging more and more beyond 15% EGR. Obviously the formulation for the laminar flame speed gives a less correct description of the real engine behavior towards the end of the combustion. However, this does not affect very much the results of the process calculation in total so that consequently a good correspondence between measurement and calculation is given over the entire technically interesting range of EGR (0% to more than 20%).

Similar to lean burn operation, the exact operating limit cannot be calculated in

the case of EGR, as there is only a steady increase in combustion time with increasing EGR.

Fig. 11 indicates the results of the calculation of nitric oxides at low partial load and with stoichiometric mixture. There is a good correspondence

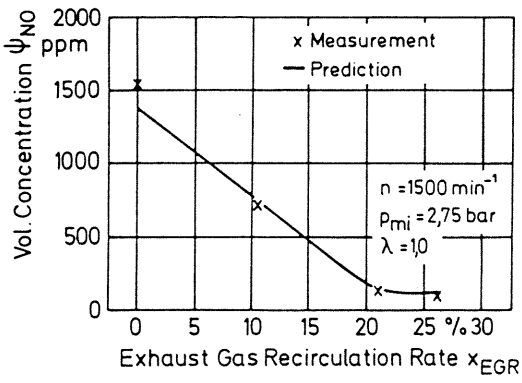

Fig. 11: Measured and calculated nitric oxide emission

of calculation and measurement over the entire range. At a rate of 10% EGR, there is a calculated and measured reduction of the nitric oxide emission by approx. 50%, at recirculation rates over 20% the reduction amounts to almost 90%. The reaction mechanism described by Kleinschmidt /4/ which implies the evaluation of 20 elementary reactions including the Zeldovich mechanism is obviously reliable with regard to the calculation of the formation process of nitric oxides in SI-engines at EGR-operation.

SUMMARY AND CONCLUSION:

The presented computer simulation program including a quasidimensional combustion model is able to describe the behavior of SI-engines under nearly all operating conditions after adapting the parameters of the turbulence model and the combustion delay. The approaches describing the laminar flame speed and the turbulence could be validated for low speeds, lean burn and EGR.

Further development of the combustion model will be carried out with regard to a better approach for the combustion delay, which is not completely sufficient at present. However, this does not affect the program`s reliability nor its practical use for the calculation of the engine process under modified conditions since the program is able to determine the optimum combustion start, but without predicting the exact spark timing.

The limits of the calculation model are equal to the limits of regular engine operation, because the effects then ocurring are not taken into account. These effects are wall quenching, flame quenching, engine misfire, unburned hydrocarbons and cycle-by-cyle variations. The latter mainly occur in the case of lean burn and EGR. With regard to low engine speeds, no limits for the combustion calculation comparable to lean burn and EGR were found.

ACKNOWLEDGEMENT:

The authors would like to thank the Deutsche Forschungsgemeinschaft (DFG, German Research) for their financial sponsorship and Prof. Dr. techn. F. Pischinger, Aachen Technical University for his valuable advice.

REFERENCES:

1. Laurenz,W., "Entwicklung und Anwendung eines Berechnungsverfahrens für den ottomotorischen Arbeitsprozeß unter Zugrundelegung einer quasi-dimensionalen Modellvorstellung", Doctor Thesis Aachen 1982

2. Blizard,N.C.,Keck,J.C., "Experimental and Theoretical Investigation of Turbulent Burning Model for Internal Combustion Engines", SAE paper 740191

3. Davis,G.C.,Borgnakke,C., "The Effect of In-Cylinder Flow Processes (Swirl, Squish and Turbulence Intensity) on Engine Efficiency - Model Predictions" SAE-paper 820045

4. Kleinschmidt,W., "Untersuchung des Arbeitsprozesses und der NO-, NO_2- und CO-Bildung im Ottomotor", Doctor Thesis Aachen 1974

5. Tabaczynski,R.J.,Ferguson,C.R., Radhakrishnan,K., "A Turbulent Entrainment Model for Spark Ignition Engine Combustion", SAE-paper 770647

6. Matsushita,S.,Inoue,T.,Nakanishi,K., "Development of the Toyota Lean Combustion System", SAE-paper 850044